

# Structural changes of diblock copolymer melts due to an external electric field: a self-consistent field theory study

Chin-Yet Lin and M. Schick

Department of Physics, University of Washington, Seattle, Washington 98195-1560

David Andelman

School of Physics and Astronomy, Raymond and Beverly Faculty of Exact Sciences,  
Tel Aviv University, Ramat Aviv 69978, Tel Aviv, Israel

(Dated: February 25, 2005)

## Abstract

We study the phase behavior of diblock copolymers in presence of an external electric field. We employ self-consistent field theory and treat the relevant Maxwell equation as an additional self-consistent equation. Because we do not treat the electric field perturbatively, we can examine its effects even when its magnitude is large. The electric field couples to the system's morphology only through the difference between the dielectric constants of the two blocks. We find that an external field aligns a body-centered cubic phase along the (111) direction, reducing its symmetry group to  $R\bar{3}m$ . Transitions between this phase and the disordered or hexagonal phases can occur for external electric fields ranging from a minimum to a maximum value beyond which the  $R\bar{3}m$  phase disappears completely. This electric-field range depends on diblock architecture and temperature. We present several cuts through the phase diagram in the space of temperature, architecture and applied field, including one applicable to a system recently studied.

## I. INTRODUCTION

Because block copolymers readily self-assemble into various ordered arrays, they have been avidly studied for technological applications such as high density porous materials, nano-lithographic templates, photonic band gap materials [1, 2, 3], and well-ordered arrays of metal nano-wires [1, 4]. One practical difficulty to their use in some applications is that the ordered phase is not created in one single crystal, but rather in domains of differing orientation. One means of aligning the domains is to apply an external electric field. It has been shown [3, 5, 6, 7, 8] that applying an electric potential, on the order of a few to a few dozen volts across electrodes separated by several micrometers, can effectively orient domains of lamellar or cylindrical morphology normal to the surfaces of thin films. The basis of this orientation effect is simple. In order to reduce accumulation of polarization charge, the system lowers its free energy by aligning cylinders or lamellae so that their long axis is parallel to the applied field.

Recently, related experiments on diblock copolymers [9] have been performed where external fields have been applied to bring about a phase transition from a phase of spheres to one of cylinders. In the phase of spheres, it is not possible to eliminate the accumulation of polarization charge so that its free energy increases in an external field with respect to a cylindrical phase, and a phase transition can be induced. This change in phase due to the application of an electric field was considered by Tsoni et al. [10], and by Xu et al [9].

The effects of an external field on an ordered array of inhomogeneous dielectric material is of great interest. First, the problem is inherently self-consistent simply because the material is a dielectric; i.e. the electric field at a given point depends upon the polarization at that point which, in turn, depends upon the local electric field. In addition, in the problem of interest here, the local dielectric constant is inhomogeneous. It depends upon the morphology of the ordered phase, which itself depends upon the local electric field [11].

In previous calculations for diblock copolymers [9, 10], this self-consistent circle has been broken by assuming that the two block are only weakly segregated, resulting in a small amplitude of the spatial variation of the relative concentration of the two blocks. In this case it follows from the vanishing of the divergence of the electric displacement that the amplitude of the spatially varying electric field is also small so that the electrostatic Maxwell equation can be solved perturbatively for the electric field as a function of the order parameter.

This procedure was carried out to quadratic order in the field by Amundson et al.[12]. It is appropriate in the weak-segregation limit, and should be adequate for determining the general phase behavior in weak external fields. However, since experiments are often not in the weak segregation limit, and the effect of electric fields has hardly been explored, further study is clearly called for.

In recent years, thermodynamic properties of block copolymer systems have been treated successfully by the full self-consistent field (SCF) theory, to which weak- and strong-segregation theories are approximations [13]. Given the self-consistent nature of an inhomogeneous dielectric in an external electric field, it seems natural to apply the full SCF theory to this problem as well. That is what we do in this paper. We solve exactly the full set of SCF equations and the appropriate Maxwell equations under the assumption of a simple constitutive relation between the local dielectric properties and the local volume fractions. In particular, we consider the evolution of the bulk phase diagram of diblock copolymers in an applied electric field, and focus upon its effect on reducing the region of the phase diagram occupied by the body-centered cubic (bcc) structure, (space group  $Im\bar{3}m$ ). Evolution of the gyroid structure (space group  $Ia\bar{3}d$ ), whose region in the phase diagram also decreases due to the application of a field, is not considered.

We calculate the strength of an external field needed to bring about a phase transition from the (distorted) spherical phase to the disordered phase and to the cylindrical phase. For the transition to the latter phase we find two distinct behaviors depending upon the architecture of the diblock, as measured by the parameter  $f_A$  introduced below. The first is brought about if a transition from the spherical phase to the cylindrical phase can be induced in the absence of an external electric field simply by reducing the temperature in the realm of interest. If so, the same must also be true for very small fields. As a consequence, one can always find a temperature in that realm at which an arbitrarily small field will induce a transition from the spherical to the cylindrical phase. The other behavior occurs if the spherical phase is the most stable one in the absence of an external field for temperatures in the realm of interest. In that case, a non-zero external field is required to induce a transition from it to the cylindrical one at any temperature in this realm. In either case, we find that for a given architecture, there is a maximum value of applied field beyond which the spherical phase is no longer the most stable one for any temperature.

In the following section, we set up the general formalism. In section III, we discuss

its application to the phase of (distorted) spheres, and compare the results of the full self-consistent calculation with those obtained from an expansion of the free energy in the electric field to order  $E^2$ . Such an expansion does not indicate the optimal direction in which the field aligns the cubic phase, whereas the full calculation shows that alignment along the (111) direction is favored over a (100) orientation. There is a concomitant reduction of the symmetry of the phase from  $Im\bar{3}m$  (bcc phase) to  $R\bar{3}m$  (distorted spherical phase). Various cuts through the phase diagram are also presented. We conclude with a brief summary and comparison with recent experiments.

## II. GENERAL FORMALISM

We consider a melt of  $n$  A-B diblock copolymer chains, each of polymerization index  $N = N_A + N_B$ . If the specific volumes of the A and B monomers are  $v_A$  and  $v_B$ , respectively, the volume per chain is  $v_p = N_A v_A + N_B v_B$ . For an incompressible melt of A-B chains, the volume fraction of the A monomers is  $N_A v_A / (N_A v_A + N_B v_B)$ , and the total system volume is  $V = n v_p$ . We assume the monomer volumes to be identical,  $v_A = v_B$ , so that the volume fraction of the A monomers is equal to the mole fraction of the A monomers,  $f_A = N_A / N$ . We also assume that the Kuhn lengths of the A and B components are identical, a length denoted  $a$ .

In the absence of an external field, the application of SCF theory [14] leads to a free energy  $F$  which is a functional of unknown fields  $W_A, W_B$ , and  $\lambda$ , and a function of temperature  $T$

$$\frac{F(W_A; W_B; \lambda; T)}{nk_B T} = \ln Q[W_A; W_B] + \frac{1}{2} \int d\mathbf{r} f(N_A, N_B, W_A, W_B, \lambda) \quad (1)$$

where  $k_B$  is the Boltzmann constant,  $\phi_A(\mathbf{r})$  and  $\phi_B(\mathbf{r})$  are the local volume fractions of A and B monomers. The dependence on  $T$  comes from the usual Flory interaction parameter,  $\chi = b/T$ , which to a good approximation is inversely proportional to the temperature,  $N = b/T$  with  $b$  a constant. The function  $Q[W_A; W_B]$  is the partition function of a single polymer chain subject to the fields  $W_A(\mathbf{r})$  and  $W_B(\mathbf{r})$ , as is given below. The field  $\lambda(\mathbf{r})$  is a Lagrange multiplier that enforces locally the incompressibility constraint,  $\phi_A(\mathbf{r}) + \phi_B(\mathbf{r}) = 1$ . The three unknown fields are determined by requiring that the free-energy functional be extremized with respect to their variation at constant  $T$ .

The fields  $W_A$  and  $W_B$  appear in the single-chain partition function of the flexible diblock copolymer,  $Q[W_A; W_B] = \int_0^1 dr q(r; 1) = c$ , where  $q(r; s)$  satisfies the modified diffusion equation

$$\frac{\partial q}{\partial s} = \frac{1}{6} N a^2 r^2 q - W_A(r) q; \quad \text{if } 0 \leq s \leq f_A; \quad (2)$$

and

$$\frac{\partial q}{\partial s} = \frac{1}{6} N a^2 r^2 q - W_B(r) q; \quad \text{if } f_A < s \leq 1; \quad (3)$$

with the initial condition  $q(r; 0) = 1$ , and  $c$  is a volume of no consequence here.

The addition of a local electric field  $E(r)$  in the derivation of the free energy  $F$  is straightforward. In an ensemble for which an external electric potential is held fixed [15], the above free energy simply becomes

$$\begin{aligned} \frac{F(W_A; W_B; T; E)}{nk_B T} = & -\ln Q[W_A; W_B] - \frac{\epsilon_0 V_p}{k_B T} \int_0^1 dr \frac{d}{dr} (r) E(r)^2 \\ & + \frac{1}{2} \int_0^1 dr f N_A W_A + f N_B W_B - (1 - f_A - f_B) g; \quad (4) \end{aligned}$$

where  $\epsilon_0$  is the vacuum permittivity, and  $\epsilon(r)$  is the local dielectric constant. A constitutive relation between  $\epsilon(r)$  and the volume fractions of A and B monomers must be specified. We choose a linear interpolation relation

$$\epsilon(r) = \epsilon_A \phi_A(r) + \epsilon_B \phi_B(r); \quad (5)$$

where  $\epsilon_A$  and  $\epsilon_B$  are the dielectric constants of pure A and B homopolymer phases, respectively. This choice is clearly correct in the limiting cases of the pure systems, and in the weak-segregation limit. It also has the virtue of simplicity and should capture the correct physics.

From the above it can be seen that a convenient scale for the strength of the electric field is

$$E = \frac{k_B T}{\epsilon_0 V_p} \quad (6)$$

The magnitude of this electric field unit at typical experimental temperatures,  $T \approx 430 \text{ K}$ , and for typical volume per polymer chain,  $v_p \approx 100 \text{ nm}^3$ , is  $E \approx 82 \text{ V/nm}$ . We shall denote the dimensionless electric field rescaled in this unit as  $\hat{E} = E/E$ . Similarly a dimensionless displacement field,  $\hat{D}$ , is conveniently defined by  $\hat{D} = \epsilon_0 E$ :

The requirement that the free energy functional be an extremum with respect to variation of  $W_A, W_B, \phi_A$ , and of the volume fractions  $\phi_A$  and  $\phi_B$  at constant temperature, or  $N$ , and fixed electric field  $\hat{E}$ , leads to the following set of SCF equations:

$$w_A = N_B + \frac{1}{2} \hat{E}^2 ; \quad (7)$$

$$w_B = N_A + \frac{1}{2} \hat{E}^2 ; \quad (8)$$

$$w_A + w_B = 1 ; \quad (9)$$

$$w_A = \frac{Q}{Q + w_A} ; \quad (10)$$

$$w_B = \frac{Q}{Q + w_B} ; \quad (11)$$

The values of  $w_A, w_B, w_A, w_B$ , which satisfy these equations are denoted by lower case letters,  $w_A, w_B, w_A, w_B$ , respectively. The free energy within the SCF approximation,  $F_{scf}$  is obtained by substitution of these values into the free energy of Eq. (4),

$$F_{scf}(T;E) = F(w_A;w_B;T;E) ; \quad (12)$$

or

$$\frac{F_{scf}}{nk_B T} = - \ln Q[w_A;w_B] - \frac{1}{2} \int dr [N_A(r) + N_B(r) + \hat{E}^2(r)] ; \quad (13)$$

In addition to these equations, there are also the Maxwell equations which the electrostatic field must satisfy in absence of free charges:

$$\nabla \cdot \hat{E} = 0 ; \quad (14)$$

$$\nabla \cdot \hat{D}(r) = \nabla \cdot (\epsilon(r)\hat{E}(r)) = 0 ; \quad (15)$$

As usual, we guarantee that the first of these equations is satisfied by introducing the electric potential  $\hat{V}(r)$ ,

$$\hat{E}(r) = - \nabla \hat{V}(r) = - \nabla V(r) = E ; \quad (16)$$

Since we will consider, in addition to the disordered phase, spatially-periodic ones, it is convenient to write all functions of position in terms of their values averaged over a unit cell

$$C_0 = \langle C \rangle = \frac{\int_{unit\ cell} C(r) dr}{\int_{unit\ cell} dr} ; \quad (17)$$

and their deviations from those average values

$$C(r) = C(r) - C_0 ; \quad (18)$$

The average values of several quantities of interest are

$$\begin{aligned}
f_{A;0} &= f_A ; \\
f_{B;0} &= 1 - f_A ; \\
\phi_0 &= \phi_A f_A + \phi_B (1 - f_A) ; \\
w_{A;0} &= N (1 - f_A) \left[ \frac{1}{2} \phi_A \hat{E}_0^2 \right] ; \\
w_{B;0} &= N f_A \left[ \frac{1}{2} \phi_B \hat{E}_0^2 \right] ;
\end{aligned} \tag{19}$$

where the value of  $\phi_0$  has been arbitrarily set to zero, and  $\hat{E}_0$  is the value of the local electric field averaged over a unit cell. To determine this without knowing the full spatially dependent electric field  $E(r)$ , we reason as follows. Assume that the external field is produced by planar electrodes which are separated by a distance  $d$  and subject to a voltage difference  $V_{12}$ . In the gap, and along the  $z$ -axis perpendicular to the electrodes, the field is  $E_{\text{ext}} = V_{12}/L$ . Given that the dielectric fills the space between the plates, and that the voltage  $V_{12}$  is held fixed as the dielectric is inserted, it follows that  $\int_0^L E_z dz = E_{\text{ext}} L$ , and that the average value of  $E_z$  is  $E_{\text{ext}}$ . We make a reasonable assumption that the free energy of the system is minimized when an axis of symmetry of one of the ordered structures coincides with the  $z$ -axis. In this case  $E_0 = \int_0^L E_z dz / L = E_{\text{ext}}$ . Hence in rescaled units

$$\hat{E}_0 = \frac{\phi_0 V_p}{k_B T} E_{\text{ext}} \hat{z} ; \tag{20}$$

and

$$\hat{E}(r) = \hat{E}(r) - \hat{E}_0 \quad r \cdot \hat{V}(r) : \tag{21}$$

Utilizing these average values, we can rewrite the free energy in the SCF approximation, Eqs. (12)-(13), in the form

$$\frac{F_{\text{scf}}}{nk_B T} = \ln \left( \frac{Q[w_A; w_B]}{Q[w_{A;0}; w_{B;0}]} \right) + N f_A (1 - f_A) \left[ \frac{1}{2} \phi_0 \hat{E}_0^2 \right] - \frac{N}{2} \int_A(r) \phi_B(r) dr ; \tag{22}$$

where, from the incompressibility condition,  $\phi_A(r) = \phi_B(r)$ . Note that the electric-field contribution  $\phi_0 \hat{E}_0^2 / 2$  is common to all phases. For the lamellar and hexagonal phases in the lowest energy orientation, this is the only contribution to the free energy from the electric field. It can conveniently be absorbed in a redefinition of the free energy

$$f_n(\hat{E}_0) = F_{\text{scf}} / nk_B T + \frac{1}{2} \phi_0 \hat{E}_0^2 : \tag{23}$$

The advantage of separating out the average values is that the only remaining Maxwell equation, Eq. (15), can be written as an inhomogeneous equation for the potential  $\hat{V}(\mathbf{r})$ ,

$$\begin{aligned} \nabla^2 \hat{V}(\mathbf{r}) &= \nabla \cdot [\mathbf{f}_A + \mathbf{f}_B(\mathbf{r})] + [\mathbf{f}_A(f_A + \mathbf{f}_A(\mathbf{r})) + \mathbf{f}_B(1 - f_A + \mathbf{f}_B(\mathbf{r}))] \nabla^2 \hat{V}(\mathbf{r}) \\ &= \hat{E}_0 \frac{\partial}{\partial z} [\mathbf{f}_A + \mathbf{f}_B(\mathbf{r})] : \end{aligned} \quad (24)$$

This, with the three remaining self-consistent equations,

$$w_A(\mathbf{r}) = N_B(\mathbf{r}) + \left( \frac{1}{2} \hat{E}_0 \nabla \hat{V}(\mathbf{r}) - (\nabla \hat{V}(\mathbf{r}))^2 \right) ; \quad (25)$$

$$w_B(\mathbf{r}) = N_A(\mathbf{r}) + \left( \frac{1}{2} \hat{E}_0 \nabla \hat{V}(\mathbf{r}) - (\nabla \hat{V}(\mathbf{r}))^2 \right) ; \quad (26)$$

$$\mathbf{f}_A(\mathbf{r}) + \mathbf{f}_B(\mathbf{r}) = 0 ; \quad (27)$$

constitute the four self-consistent equations which determine the four functions  $w_A(\mathbf{r})$ ,  $w_B(\mathbf{r})$ ,  $\mathbf{f}_A(\mathbf{r})$ , and  $\hat{V}(\mathbf{r})$ .

We note that with our choice of constant external field applied along the  $z$  direction, the Maxwell equation, Eq. (24), admits the following symmetry:

$$\begin{aligned} \hat{V}(\mathbf{r}_?; z) &= \hat{V}(\mathbf{r}_?; z) = \hat{V}(\mathbf{r}_?; -z) \\ \mathbf{f}_A(\mathbf{r}_?; z) &= \mathbf{f}_A(\mathbf{r}_?; z) + \mathbf{f}_B(\mathbf{r}_?; z) \\ &= \mathbf{f}_B(\mathbf{r}_?; z) = \mathbf{f}_A(\mathbf{r}_?; -z) ; \end{aligned} \quad (28)$$

where the components of  $\mathbf{r}$  have been written as  $(\mathbf{r}_?; z)$ . The self-consistent equations, Eq. (24)–(27), are now solved by a standard procedure of expanding the functions of position in a complete set of functions with the above symmetries and those of any specific phase considered [13]. We have utilized in our calculation sets of basis functions containing between 70 and 125 functions, depending upon the value of  $N$ .

The only parameters entering our calculation are  $N$ ,  $f_A$ ,  $\mathbf{f}_A$  and  $\mathbf{f}_B$ , and the rescaled external field  $E_{\text{ext}} = E$ . Comparison of the results with experiment requires the evaluation of  $E$  for given  $T$  and volume per chain  $v_p$ . In addition, the relation between  $T$  and  $N$  must be specified.

### III. RESULTS

As noted earlier, the free energies of lamellar or hexagonal phases are minimized when the lamellae or the cylinders are aligned parallel to the electric field because in this orientation



there is no buildup of polarization charge. In the body-centered cubic (bcc) phase, however, there must be an accumulation of polarization charge irrespective of the external field direction. We must determine which field direction produces a phase of distorted spheres with the lowest free energy, and how large a field this phase can sustain before a transition to the hexagonal phase is encountered. It is these issues which we now address.

#### A. The $R\bar{3}m$ to Hexagonal phase transition

The symmetry group of the bcc phase is  $Im\bar{3}m$  which has three two-dimensional space subgroups:  $p4mm$  along the  $[100]$  direction,  $p6mm$  along the  $[111]$  direction, and  $p2mm$  along the  $[110]$  direction. If the field were applied along either the  $[110]$  or  $[100]$  directions the symmetry would be reduced to  $I4mm$ , while if it were applied along the  $[111]$  direction, the symmetry would be reduced to  $R\bar{3}m$ . The symmetry in the latter case is of a bcc arrangement of spheres that has been distorted along the  $[111]$  direction. As the  $R\bar{3}m$  group has the  $p6mm$  symmetry of the hexagonal phase, one would suspect that a field applied along the diagonal  $[111]$  direction will result in the lowest free energy. By direct calculation of these configurations, we find that the  $R\bar{3}m$  phase does indeed have a lower free energy than that of the  $I4mm$ .

That the electric field favors one orientation of the  $Im\bar{3}m$  over another is an effect which is not captured by an expansion of the free energy to quadratic order in the external field  $[11]$ . Nonetheless it is instructive to consider the result of such an expansion. It is obtained by solving the Maxwell equation  $\nabla \cdot (\epsilon_A + \epsilon_B)E = 0$  to second order in  $E$  to obtain  $E(\epsilon_A + \epsilon_B)$ ; and evaluating this field from the volume fractions characterizing the system in the absence of an external field. The distortion of the density distribution produced by this field itself contributes terms to the free energy which are higher order in  $E^2$ . For a phase which is cubic in the absence of an electric field, the perturbation result can be written as [12]

$$\frac{F_{\text{pt}}(\hat{E}_0)}{nk_B T} = \frac{1}{2} \epsilon_0 \hat{E}_0^2 - \frac{1}{12} \frac{\epsilon_A - \epsilon_B}{\epsilon_0} \epsilon_0^2 \int d\mathbf{r} [\epsilon_A(\mathbf{r}) - \epsilon_B(\mathbf{r})]^2; \quad (29)$$

$$+ \frac{1}{2} \epsilon_e \hat{E}_0^2;$$

where  $\epsilon_A - \epsilon_B$  is the variation of the local volume fraction in the zero-field structure,

and  $\epsilon_e$  is, by definition, the effective dielectric constant for the structure in the field.

We now compare the full SCF solution with this perturbation result. We choose  $N = 15$  and  $f_A = 0.29$ , values at which the bcc phase is the most stable in zero electric field. The dielectric constants are chosen to make contact with recent experimental systems of polymethylmethacrylate (PMMA)/polystyrene (PS) diblock copolymer, which is referred to hereafter as the PMMA-PS system. At experimental temperatures around 160 °C the dielectric constants appropriate to the PMMA-PS copolymer with PMMA being the A block and PS the B block are:  $\epsilon_A = 6.0$  (for PMMA), and  $\epsilon_B = 2.5$  (for PS) [5, 9, 10] which yield an average of  $\epsilon_0 = 3.52$ . In Fig. 1, we show the difference,  $f_n$ , between the free energy  $f_n(\hat{E}_0) = F_{scf} - nk_B T + \epsilon_0 \hat{E}_0^2/2$ , Eq. (23), and its value in zero external field in the bcc phase. It is shown as a function of  $\hat{E}_0$ , for the hexagonal phase and for the R3m phase, as calculated from the full SCF theory and from perturbation theory. The latter is seen to be adequate for fields smaller than ten to twenty percent of the natural unit  $E$  at which  $\hat{E}_0 = 1$ . The figure also shows that there is a transition from the R3m to the hexagonal phase at a value of  $\hat{E}_0 = 0.477$  as determined from the full self-consistent calculation. Perturbation theory underestimates the magnitude of the field needed to bring about this transition. That the transition is first-order is easily seen as follows. The average electric and displacement fields,  $E_0$  and  $D_0$ , are evaluated by taking their spatial averages over the unit cell. In our case the only non-zero average components are those in the z-direction, and they are related to the free energy per unit volume according to

$$\frac{\partial F}{\partial E_0} = D_0 ; \quad (30)$$

or

$$\frac{\partial F - nk_B T}{\partial \hat{E}_0} = \hat{D}_0 : \quad (31)$$

One sees from Fig. 1 that at the phase transition, the free energies of the R3m and hexagonal phases intersect with different slopes, therefore the displacement field changes abruptly.

As a result of the application of the electric field along the [111] direction, the spheres of minority component are elongated in this direction. A density profile of the system in the R3m phase at an external field  $\hat{E}_0 = 0.470$ , slightly smaller than that at the transition to the hexagonal phase,  $\hat{E}_0 = 0.477$ , is shown in Fig. 2 (b). At the transition, the profile changes abruptly to that of the hexagonal phase, which is also shown in 2 (c) for  $\hat{E}_0 = 0.480$ . To see the extent of the distortion in the R3m phase, which can be characterized by the

aspect ratio of the distorted spheres, 1.248, we also present the density profile of the bcc phase in zero external field, in 2(a). The cuts are in the plane containing the [111] and [110] directions.

There are two features of interest that can be seen particularly clearly from the approximate expression of Eq. (29). The first is that in the R3m phase, the effective average dielectric constant,  $\epsilon_e$ , is smaller than  $\epsilon_0$ . In the hexagonal and disordered phases, however,  $\epsilon_e$  is precisely  $\epsilon_0$ . Therefore, the displacement field  $D_0$  in the R3m phase is smaller than in the other two phases. This is in accord with the change of slope of the free energy with electric field shown in Fig.1 and Eqs. (30)–(31).

The second concerns the fact that the dielectric constants are temperature dependent. Therefore, the value of the electric field needed to bring about a phase transition will also vary with temperature. The perturbation expression leads one to expect that, for fields smaller or comparable to  $E_c$ , the natural  $E_c$ -field scale, the field at the transition will vary as

$$E_{tr}(T) / \frac{[\epsilon_0(T)]^{1/2}}{\epsilon_A(T) \epsilon_B(T)} = \frac{[\epsilon_A \epsilon_A(T) + (1 - \epsilon_A) \epsilon_B(T)]^{1/2}}{\epsilon_A(T) \epsilon_B(T)} ; \quad (32)$$

B. The generalized Clausius-Capeyron equation

Before presenting the phase diagram of our A/B block copolymer system in an  $E$ -field, we will make use of some general thermodynamic considerations. In particular, from the differential of the free energy per unit volume

$$d(F/V) = -s dT - D_0 dE_0 ; \quad (33)$$

where  $s = S/V$  is the entropy per unit volume, one immediately derives a Clausius-Capeyron equation for the slope of the coexistence line between any two phases

$$\frac{dE_0}{dT} = - \frac{s}{D_0} ; \quad (34)$$

where  $s$  and  $D_0$  are the differences in entropies and displacement fields, respectively, in the coexisting phases. This can be expressed in terms of  $\hat{E}_0$ ,  $\hat{D}_0$  and  $N = b/T$  as

$$\frac{d\hat{E}_0}{d(N)} = \frac{v_p}{N} \frac{(s/k_B)}{\hat{D}_0} + \frac{\hat{E}_0}{2N} ; \quad (35)$$

## C . Phase diagrams

We now turn to the phase diagram as a function of the inverse temperature,  $N$ , the A-monomer fraction,  $f_A$ , and the applied external field,  $\hat{E}_0 = E_0/E$ . We concentrate on the portion of the phase diagram involving the phase with  $R\bar{3}m$  symmetry and the neighboring disordered and hexagonal phases. In the space of inverse temperature  $N$ , the fraction  $f_A$ , and applied field, the  $R\bar{3}m$  phase occupies a volume which is bounded by two sheets of first-order transitions: one from the  $R\bar{3}m$  to the hexagonal phase, the other from the  $R\bar{3}m$  to the disordered phase. These two sheets of first-order transitions meet at a line of triple points,  $[\hat{E}_{0;\text{triple}}(f_A), N_{\text{triple}}(f_A)]$ . Beyond this line, the  $R\bar{3}m$  phase no longer exists, while the disordered and hexagonal phases remain. They are separated by another sheet of first-order transitions which emerges from the line of triple points. Hence this line is the locus at which all three sheets of first-order transitions meet.

In Fig. 3 we show a cut through the phase diagram at fixed A-monomer fraction,  $f_A = 0.29$ . The cut shows the phase diagram as a function of the dimensionless electric field  $\hat{E}_0$  and  $N$ . At zero external field, the entropy difference between the bcc phase and the hexagonal phase is non-zero, but the difference in displacement field obviously vanishes. From the Clausius-Clapeyron equation, Eq. (35), the slope of the phase boundary between these two phases must be infinite at zero  $E$ -field. The same is true for the slope of the phase boundary between the bcc phase and the disordered phase at vanishing  $E$ -fields. Furthermore, we know from the zero electric field results that the entropy of the disordered phase is greater than that of the bcc phase which, in turn, is greater than that of the hexagonal phase. We also know that the displacement field in the disordered and in the hexagonal phases is equal to  $\epsilon_0 E_0$ . As we noted earlier, the displacement field in the  $R\bar{3}m$  phase is less than this value. This information, together with the Clausius-Clapeyron, Eq. (35), implies that the phase boundary between  $R\bar{3}m$  and the disordered phase has a negative slope, while that between  $R\bar{3}m$  and the hexagonal phase is positive in accord with Fig. 3.

Moreover, because of the presence of the positive second term in Eq. (35), the positive slope of the phase boundary between disordered and  $R\bar{3}m$  phases will be greater in magnitude, or steeper, than that between the  $R\bar{3}m$  and hexagonal phases. This is borne out by Fig. 3. The three phases meet at the triple point, above which the phase boundary is vertical as there is no difference between the displacement fields of the coexisting disordered

and hexagonal phases. The value of the electric field at the triple point is  $\hat{E}_{0,\text{triple}} = 0.71$ .

To make contact with experiment, we take parameters to fit the PMMA-PS system of Ref [4]. With  $f_A = 0.29$  and a molecular mass of  $3.9 \cdot 10^4 \text{ g/mol}$ , and utilizing the known values of monomeric volumes, we obtain a chain length of  $N = 379$  and a volume per PMMA-PS chain of  $v_p = 61.24 \text{ nm}^3$ . At  $T = 430 \text{ K}$  this yields  $E = (k_B T =_0 v_p)^{1/2} = 104.6 \text{ V/m}$ . Therefore, the value of the electric field at the triple point is in physical units  $E_{0,\text{triple}} = 74.5 \text{ V/m}$  at this value of  $f_A$  and  $T$ . One sees from the figure that a transition from R3m to hexagonal phases could be brought about at electric fields within the interval from this maximum value down to zero, depending upon the values of  $N$  and  $f_A$ .

The evolution of the phase diagram of Fig. 3 with A-monomer fraction,  $f_A$ , is easily understood. As  $f_A$  decreases from 0.29, the phase boundary at zero field between R3m and hexagonal phases moves toward greater values of  $N$  as does the boundary between disordered and R3m phases. When  $f_A$  is smaller than  $f_A^{\text{coex}} = 0.114$ , the value at which the bcc and hexagonal phases coexist at infinite  $N$  [16], the boundary between hexagonal and R3m phases will asymptote with zero slope to an  $f_A$ -dependent finite value as  $N$  increases without limit. This zero slope also follows from the Clausius-Capeyron equation (35) due to the fact that the ratio  $s = D_0^*$  is finite and  $1 = N \rightarrow 0$ .

An example of such a phase diagram is shown in Fig. 4. This figure corresponds to a system with  $f_A = 0.1 < f_A^{\text{coex}} = 0.114$ , as was investigated recently in Ref. [9]. In contrast with Fig. 3, one sees here that the interval over which a transition can be observed from R3m to hexagonal phases now extends from the triple point at  $\hat{E}_0 = 2.56$  down to a non-zero minimum value of  $\hat{E}_0 = 1.33$ . That is, for electric fields less than this minimum value, no transition from the R3m to a hexagonal phase occurs within our model. For PMMA-PS with  $f_A = 0.1$ , and molecular mass of  $1.51 \cdot 10^5 \text{ g/mol}$ , as in Ref. [9], we obtain  $N = 1458$  and a volume per chain  $v_p = 239.7 \text{ nm}^3$ . Therefore at the experimental temperature of  $T = 430 \text{ K}$ , the unit of electric field  $E = 52.9 \text{ V/m}$ . In physical units, then, the triple point occurs at an external field of about  $135 \text{ V/m}$  and the minimum electric field needed to produce a transition can be estimated to be  $79 \text{ V/m}$ .

In Fig. 5 we show a different cut through the phase diagram in the  $(\hat{E}_0, f_A)$  plane and for a fixed  $N = 13.3$ . The location of the triple point is  $\hat{E}_{0,\text{triple}} = 0.58$  and  $f_{A,\text{triple}} = 0.320$ . This figure, and that of Figs. 3 and 4, show that the value of the electric field needed to bring about a transition from the R3m phase is, for a given  $f_A$  fraction, a sensitive function

of temperature and, for a given temperature, a sensitive function of the mole fraction of A block,  $f_A$ .

Figure 6 shows two cuts through the phase diagram at constant electric field,  $\hat{E}_0 = 0$ , and  $\hat{E}_0 = 0.2$ . The solid line at lower  $N$  shows the phase boundary at zero-field between disordered and bcc phases while the solid line at larger  $N$  shows the zero-field phase boundary, between the bcc and hexagonal phases. The dashed lines between them show the phase boundaries for  $\hat{E}_0 = 0.2$ . The line denoted B is the boundary between the disordered and the  $R\bar{3}m$  phase of distorted spheres, A is the boundary between  $R\bar{3}m$  and hexagonal phases. These boundaries meet at the triple point,  $tr$ , which occurs at  $N = 11.43$ , and  $f_A = 0.39$ . For larger values of  $f_A$ , there is a line, C, of transitions directly from the disordered to the hexagonal phase. As the external field increases still further, the triple point recedes to larger values of  $N$  leaving behind only the line of direct transitions between disordered and hexagonal phases. Note that, except for the location of its terminus at the triple point, this boundary is independent of the applied field as it contributes to the free energy of both of these phases equally. The dielectric constants used to generate this figure are the same as those used in previous figures.

For completeness, we have also examined the case in which the dielectric constants of the minority and majority components are interchanged as compared with Fig. 3. Namely, the majority component with,  $f_A = 0.71$  has the larger dielectric constant of  $\epsilon_A = 6.0$  and the minority the smaller value of  $\epsilon_B = 2.5$ . We find that the  $R\bar{3}m$  phase is now somewhat more stable with respect to the hexagonal phase, so that the value of the external electric field needed to bring about a transition from the former to the latter phase is increased. We note that this interchange increases the average value of the dielectric constant, so that all phases have a lower free energy due to the factor of  $\epsilon_0 \hat{E}_0^2 = 2$  which it contains. However, it is not a priori obvious that the  $R\bar{3}m$  phase would have its free energy lowered by more than that of the hexagonal phase by this interchange. In addition, we have determined that the spheres of minority component and lower dielectric constant distort in the  $[111]$  direction just as in the case when the minority component has the larger dielectric constant. The above effects are not captured by the perturbation result of Eq. (29) which is invariant under the interchange of  $\epsilon_A$  and  $\epsilon_B$ .

#### IV . C O N C L U D I N G R E M A R K S

In sum , we have calculated the phase diagram of a block copolymer system in an external electric field which couples to the diblocks through the difference in their dielectric constants. We have employed a fully self-consistent field approach in which the relevant Maxwell equation is treated on an equal footing with the other self-consistent equations. We have determined that the body-centered cubic phase will preferentially align along the  $[111]$  direction causing its symmetry to be reduced to  $R\bar{3}m$  . The electric field can induce phase transitions between this phase and either the disordered or the hexagonal phase. The strength of the field needed to induce such transitions is a sensitive function of the parameters of the system , such as its temperature and its chain architecture, which in the case of linear diblocks is quantified simply by the mole fraction,  $f_A$  .

For parameters that fit the experimental PMMA-PS diblock copolymer system investigated recently [9]:  $f_A = 0.1$ ,  $v_p = 239.7 \text{ nm}^3$ , and  $T = 430 \text{ K}$ , we find that an electric field of at least  $70 - 80 \text{ V / m}$  would be needed to observe a transition to the hexagonal phase. This contrasts with the reported existence of such a phase transition under an applied field of only  $40 \text{ V / m}$  . There are several possible explanations of the difference between the experimental results and the theoretical ones presented here.

Our model employs a linear constitutive relation between dielectric constant and volume fractions, and characterizes the PMMA-PS system by a few general parameters, the PMMA mole fraction  $f_A$  , and the interaction parameter  $\chi$  . It further assumes equal volumes for both monomers and equal Kuhn lengths for them . One knows that deviations from the last assumption certainly shift the locations of the phase boundaries [17]. It is plausible that at rather asymmetric volume fractions of  $f_A = 0.1$ , the model provides only semi-quantitative agreement with the experimental PMMA-PS phase diagram . Any difference in the theoretical and experimental phase diagrams at zero electric field will, in the presence of a non-zero one, manifest itself in a difference in relative stability of the various phases. Given the sensitive dependence on the phase boundaries of the minimum external field needed to bring about a phase transition, differences between the general theory and the experimental result are to be expected. At present, the phase diagram of the PMMA-PS system of Ref. [9] is not yet known . When additional experimental information becomes available, one will also need to determine the relationship between the temperature and the  $\chi$  interaction

parameter in order to convert the phase diagram calculated here to practical units so that it can be compared directly to the experimental one.

Lastly, we have employed a simple coupling between the system and the external field via the difference in dielectric constants of the copolymer blocks. Other couplings are possible [18, 19]. Just such an additional coupling, to mobile ions, has been suggested by Tsori et al. [10] and is discussed also in Ref. [9]. A minute fraction of mobile ions embedded in the minority PMMA fraction and not in the majority PS can lead to an enhanced response of the PMMA-PS system to external electric fields with moderate magnitude. It could also change the phase diagram quantitatively resulting in a substantial lowering of the triple-point value of the electric field. Additional experiments, particularly on copolymers with the same PMMA-PS blocks, but at different temperatures or values of the architectural parameter  $f_A$ , would be most useful to shed additional light on the comparison of theory and experiment. In particular, a comparison of the two PMMA-PS systems of Ref. [4] and Ref. [9] would be enlightening because, as Figs. 3 and 4 show, they are predicted here to exhibit significantly different phase behavior in an external electric field.

#### Acknowledgment

We are indebted to Ludwik Leibler, Tom Russell, Yoav Tsori and Ting Xu for illuminating exchanges. Partial support from the National Science Foundation under grant No. 0140500, the National Science Foundation IGERT fellowship from the University of Washington Center of Nanotechnology, the United States-Israel Binational Science Foundation (BSF) under grant No. 287/02 and the Israel Science Foundation under grant No. 210/01 is gratefully acknowledged.



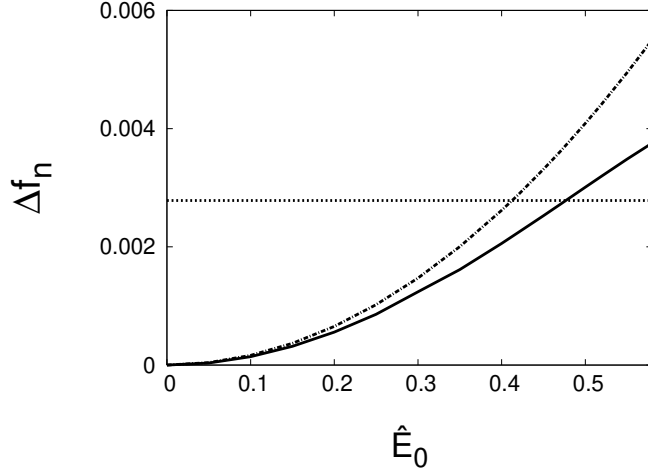


FIG .1: The difference,  $\Delta f_n$ , between the dimensionless free energy,  $f_n$ , defined in Eq. (23) and its value in zero external field in the bcc phase. It is calculated from the SCF theory, and is plotted versus dimensionless external electric field,  $\hat{E}_0 = E_0/E$ , for the hexagonal phase (horizontal dotted line) and the R3m phase (solid line). The system is characterized by a  $N = 15$ ,  $f_A = 0.29$ . The dielectric constants are:  $\epsilon_A = 6.0$  (for the PMMA block), and  $\epsilon_B = 2.5$  (for the PS block), yielding  $\epsilon_0' = 3.52$ . The perturbation theory result for the R3m phase is shown as a dashed and dotted line. It has a higher free energy.

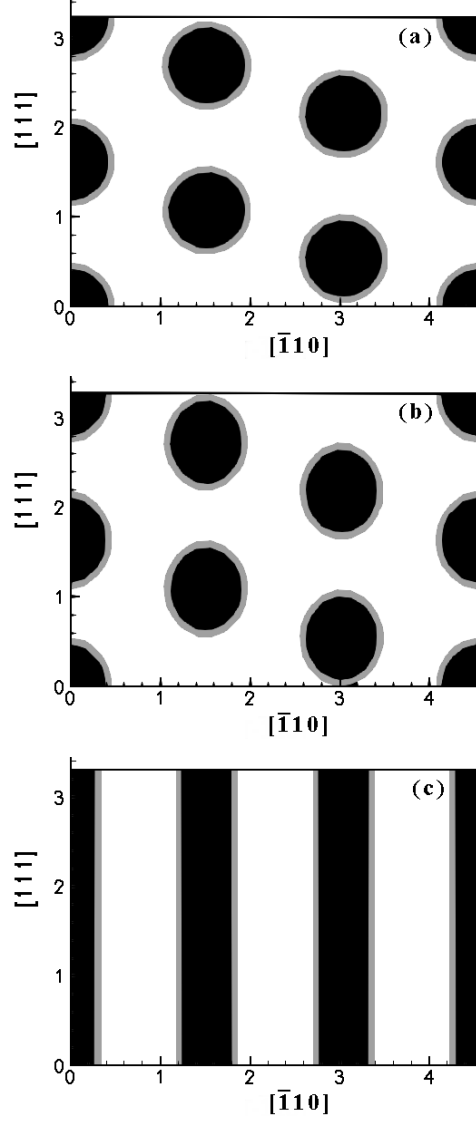


FIG. 2: Density profiles for three different phases of a system characterized by  $N = 15$  and  $f = 0.29$ , with other parameters as in Fig. 1. (a) the bcc phase which occurs in zero external field; (b) the  $R\bar{3}m$  phase at an external electric field  $\hat{E}_0 = 0.470$  just below the phase transition to the hexagonal phase which occurs at  $\hat{E}_0 = 0.477$ ; (c) the hexagonal phase, which is shown for  $\hat{E}_0 = 0.480$ . The cuts are in the plane containing the  $[111]$  and  $[\bar{1}10]$  directions. In the black regions, the local volume fractions of component A is greater than 0.55, in the intermediate regions, it is between 0.55 and 0.45, and in the white regions, it is less than 0.45.

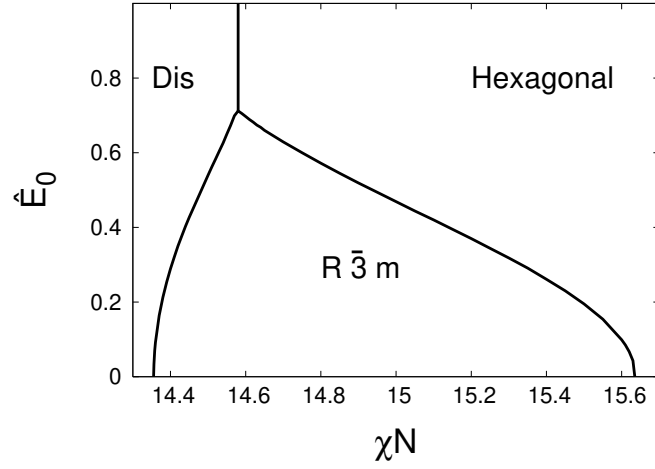


FIG . 3: Calculated phase diagram of a diblock copolymer with a volume fraction of  $f_A = 0.29$  in the presence of an external electric field. The phase diagram is shown as a function of the dimensionless field  $\hat{E}_0$  and the interaction parameter  $N$ . The triple point is located at  $\hat{E}_{0,\text{triple}} = 0.71$ ,  $N = 14.58_{\text{triple}}$ . Other parameters as in Fig. 1.

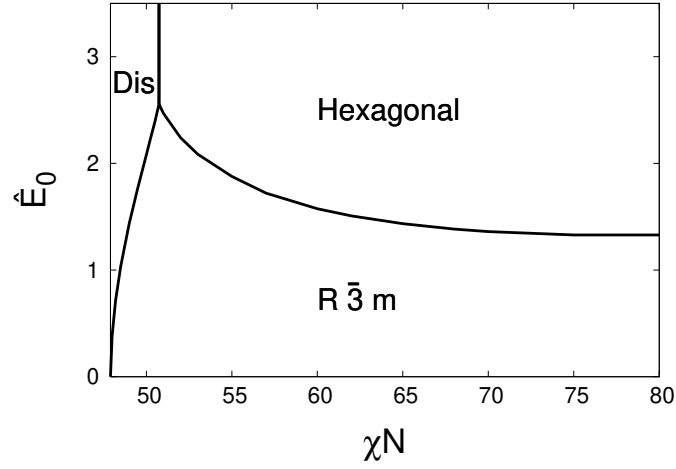


FIG . 4: Calculated phase diagram of a diblock copolymer in the presence of an external electric field. Similar to Fig. 3 but with fraction of the A block,  $f_A = 0.1$ . The phase diagram is shown as a function of the dimensionless field  $\hat{E}_0$  and the interaction parameter  $\chi N$ . The triple point is located at  $\hat{E}_{0,\text{triple}} = 2.56$ ,  $N_{\text{triple}} = 50.74$ .

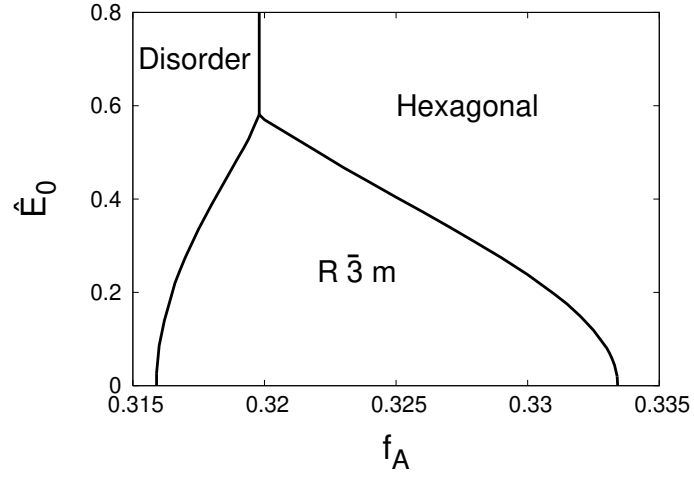


FIG .5: Calculated phase diagram for a diblock copolymer as a function of dimensionless external field and the A mole fraction parameter,  $f_A$ . Other parameters are  $N = 133$ ,  $\chi_A = 6.0$  and  $\chi_B = 2.5$ . The triple point occurs at  $\hat{E}_{0,\text{triple}} = 0.58$  and  $f_{A,\text{triple}} = 0.32$ .

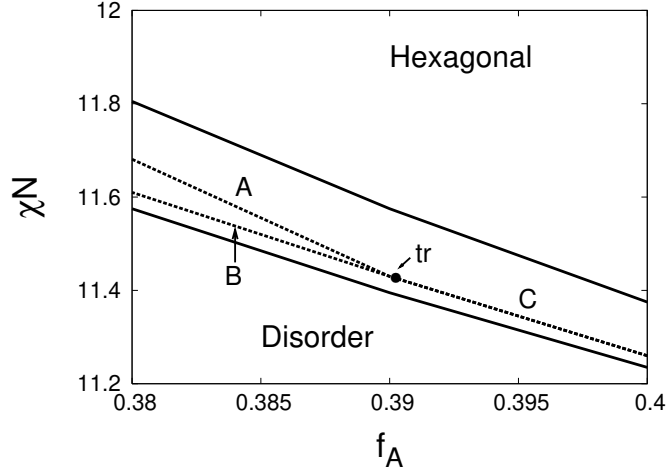


FIG . 6: Calculated phase diagram at constant electric eld,  $\hat{E}_0$ . The outer two solid lines are the  $E_0 = 0$  disorder-to-bcc and bcc-to-hexagonal phase boundaries. Between them we show three other transition lines for  $\hat{E}_0 = 0.2$ . They are the R3m -to-Hexagonal, (A), R3m -to-D isorder (B), and D isorder-to-H exagonal transition (C). These three lines meet at tr, the triple point:  $f_{A \text{ triple}} = 0.390$  and  $N_{\text{triple}} = 11.43$ .

- 
- [1] Park, M .; Harrison, C .; Chaikin, P.M .; Register, R .A .; Adamson, D .H ., Science 1997, 276, 1401.
  - [2] Walheim, S .; Schaer, E .; Mlynsek, J.; Steiner, U ., Science 1999, 283, 520.
  - [3] Morkved, T .; Lu, M .; Urbas, A .M .; Ehrichs, E .E .; Jaeger, H .M .; Mansky, P .; Russell, T .P ., Science 1996, 273, 931.
  - [4] Thum-Albrecht, T .; Schotter, J.; Kastle, G .A .; Emley, N .; Shibauchi, T .; Krusin-Elbaum, L .; Guarini, K .; Black, C .T .; Tuominen, M .T .; Russell, T .P ., Science 2000, 290, 2126.
  - [5] Thum-Albrecht, T .; DeRouchey, J.; Russell, T .P ., Macromolecules 2000, 33, 3250.
  - [6] Boker, A .; Knoll, A .; Eils, H .; Aebetz, V .; Muller, A .H .E .; Krausch, G ., Macromolecules 2002, 35, 1319.
  - [7] Boker, A .; Eils, H .; Hansel, H .; Knoll, A .; Ludwigs, S .; Zettl, H .; Zvelindovsky, A .; Sevink, G .J.A .; Urban, V .; Muller, A .H .E .; Krausch, G ., Macromolecules 2002, 35, 1319.
  - [8] Tsoni, Y .; Andelman, D ., Macromolecules 2002, 35, 5161.
  - [9] Xu, T .; Zvelindovsky, A .; Sevink, G .; Gang, O .; Ocko, B .; Zhu, Y .; Gido, S .; Russell, T .P ., Macromolecules 2004, 37, 6980.
  - [10] Tsoni, Y .; Toumilhac, F .; Andelman, D .; Leibler, L ., Phys. Rev. Lett. 2003, 90, 145504.
  - [11] Amundson, K .; Helfand, E .; Quan, X ., Macromolecules 1994, 27, 6659.
  - [12] Amundson, K .; Helfand, E .; Quan, X ., Macromolecules 1993, 26, 2698.
  - [13] Matsen, M .W .; Schick, M ., Phys. Rev. Lett. 1994, 72, 2660.
  - [14] Schmid, F ., J. Phys.-Condensed Matter 1998, 10, 8105.
  - [15] Landau, L .; Lifshitz, E .; Pitaevskii, L ., Electrodynamics of Continuous Media, Pergamon Press, Oxford 1984.
  - [16] Matsen, M .W .; Whitmore, M ., J. Chem. Phys. 1996, 105, 9698.
  - [17] Matsen, M .W .; Schick, M ., Macromolecules 1994, 27, 4014.
  - [18] Gurovich, E ., Macromolecules 1994, 27, 7063.
  - [19] Onuki, A .; Fukuda, J.-i., Macromolecules 1995, 28, 8788.